SZABO SCANDIC

Part of Europa Biosite

Produktinformation

- Forschungsprodukte & Biochemikalien
- Zellkultur & Verbrauchsmaterial
- Diagnostik & molekulare Diagnostik
- Laborgeräte & Service

Weitere Information auf den folgenden Seiten!
See the following pages for more information!

Lieferung & Zahlungsart

siehe unsere Liefer- und Versandbedingungen

Zuschläge

- Mindermengenzuschlag
- Trockeneiszuschlag
- Gefahrgutzuschlag
- Expressversand

SZABO-SCANDIC HandelsgmbH

Quellenstraße 110, A-1100 Wien

T. +43(0)1 489 3961-0

F. +43(0)1 489 3961-7

mail@szabo-scandic.com

www.szabo-scandic.com

linkedin.com/company/szaboscandic

Order online now!

www.rockland.com
tech@rockland.com
+1 484.791.3823

Datasheet for 18-8817-30

Mouse TrueBlot® ULTRA: Anti-Mouse Ig HRP

Overview

Description:	Mouse TrueBlot® ULTRA: Anti-Mouse Ig HRP - 18-8817-30
Item No.:	18-8817-30
Size:	20 µL
Applications:	ELISA, IP, WB, Biochemical Assay, ChIP, IF
Reactivity:	Mouse
Host Species:	Rat

Product Details

Background:	Mouse IgG TrueBlot® ULTRA is a unique Anti-Mouse IgG monoclonal secondary antibody. Mouse IgG TrueBlot® ULTRA enables detection of immunoblotted target protein bands, without hindrance by interfering immunoprecipitating immunoglobulin heavy and light chains. It is easy to generate publication-quality IP/Western blot data with Mouse IgG TrueBlot® ULTRA, simply substitute the conventional Anti-Mouse IgG blotting reagent with Mouse IgG TrueBlot® ULTRA and follow the prescribed protocol for sample preparation and immunoblotting. Mouse IgG TrueBlot® ULTRA is ideal for use in protocols involving immunoblotting of immunoprecipitated proteins. Mouse IgG TrueBlot® ULTRA preferentially detects the non-reduced form of mouse IgG (IgG1, IgG2a, IgG2b, IgG3) over the reduced, SDS-denatured form of IgG. When the immunoprecipitate is fully reduced immediately prior to SDS-gel electrophoresis, reactivity of Mouse IgG TrueBlot® ULTRA with the 55 kDa heavy chains and the 23 kDa light chains of the immunoprecipitating antibody is minimized thereby eliminating interference by the heavy and light chains of the immunoprecipitating antibody in IP/immunoblot applications. Applications include studies examining post-translational modification (e.g., phosphorylation or acetylation) or protein-protein interactions.
Synonyms:	Anti-Mouse IgG HRP, TrueBlot, HRP TrueBlot ULTRA, Peroxidase TrueBlot, TrueBlot for IP/WB, TrueBlot for immunoprecipitation, TrueBlot for western blotting
Host Species:	Rat
Conjugate:	Peroxidase (HRP) ULTRA
Clonality:	Monoclonal
Clone ID:	eB144
Format:	IgG

Target Details

Reactivity:	Mouse
Purity/Specificity:	Mouse TrueBlot® ULTRA Antibody Peroxidase Conjugate was prepared from tissue culture supernatant by Protein G affinity chromatography. Assay by immunoelectrophoresis resulted in a single precipitin arc against Anti-Mouse Serum. Reactivity is observed against native Mouse IgG by both Western blot and ELISA.
Relevant Links:	• TrueBlot HRP Product Protocols • TrueBlot IP Set Protocol

Application Details

Tested Applications:	ELISA, IP, WB
Suggested Applications:	Biochemical Assay, ChIP, IF (Based on references)
Application Note:	Mouse TrueBlot® ULTRA has been tested in ELISA, IP, and Western blot and may also be used for detection in immunoblotting assays that do not employ immunoprecipitation. Mouse IgG TrueBlot® ULTRA is provided as 1000X solution. To achieve best results when detecting mouse IgG1 subtypes, we recommend performing a dot blot or titration to determine the optimal dilution factor for your desired application. All recommended dilutions for listed applications are intended as an initial recommendation, specific conditions for each protein and antibody combination should be specifically optimized by the end user. In order to conserve reagent, we recommend incubating the blots from minigels in sealed bags (removing as much air as possible) with minimal volume (2-3 mLs). If used conservatively at 2.5mls/blot will yield enough reagent for 8 blots. Note that there are three key procedural considerations: 1. Protein A or G beads may be used with the mouse, goat and sheep TrueBlot secondaries, but not with the rabbit TrueBlot secondary. Use of protein A or G beads with the rabbit TrueBlot will result in contaminating bands. 2. Immunoprecipitate should be completely reduced. 3. BLOTTO/Milk should be used as the blocking protein for the immunoblot.
Assay Dilutions:	All assays should be optimized by the user. Recommended dilutions (if any) may be listed below.
IF:	User Optimized
IP:	User Optimized
WB:	1:1000

Formulation

Physical State:	Liquid (sterile filtered)

Concentration:	1.0 mg/mL
Buffer:	0.02 M Potassium Phosphate, 0.15 M Sodium Chloride, pH 7.2
Preservative:	Proclin is added as an antimicrobial agent.
Stabilizer:	0.1 mg/ml Bovine Serum Albumin (BSA) - IgG and Protease free, 50% (v/v) Glycerol

Shipping & Handling

Shipping Condition:	Wet Ice
Storage Condition:	Store at -20°C. This product is guaranteed for 6 months upon receipt, when handled and stored as instructed.
Expiration:	Expiration date is six (6) months from date of receipt.

Images

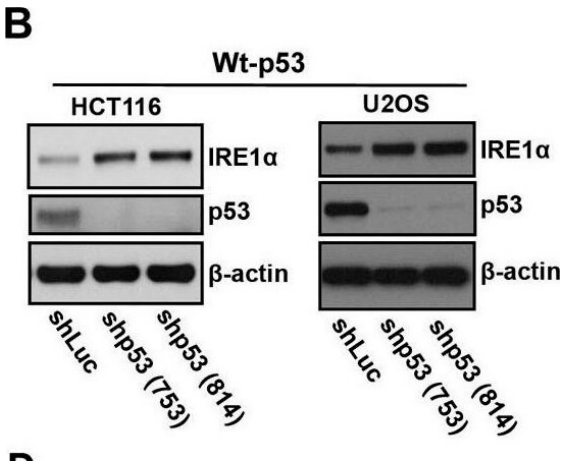

Western Incubation Box

IRE1α expression is regulated by p53. A.) Western blot analysis of the expression of endogenous IRE1α in 23 human cancer cell lines. Cell lines were grouped according to expression of wild-type or mutant p53 as indicated. (A well between wt-p53 and mutant-p53 cell lines was cut, from the gel as indicated by a black line, due to the controversial p53 status of the cell line). Right panel: The intensities of the IRE1α bands (left panel) are expressed relative to those of β-actin. Values shown are the mean ± standard deviation (s.d.). The P value was calculated using two-way ANOVA. B.) Downregulation of p53 expression induces increased expression of IRE1α. HCT116 p53+/+ and U2OS cells were transfected with shLuc, shp53 (753), or shp53 (814), and selected using puromycin. Whole cell lysates of a pool of transfectants were analyzed using western blotting with the indicated antibodies. C.) Overexpression of wild-type p53 inhibits IRE1α expression in mutant-p53 cell lines. Cell lysates, prepared 48 h after transfection with wild-type p53, were analyzed for the expression of indicated proteins. D.) Mutant p53 proteins do not inhibit IRE1α expression. Cell lysates were prepared from cells transfected with p53-G245S, p53-R248W, p53-249S, and p53-R273H expression vectors or from cells that constitutively expressed wild-type p53 and were analyzed for the expression of the indicated proteins. Figure provided by CiteAb. Source: Oncotarget, PMID: 26254280.

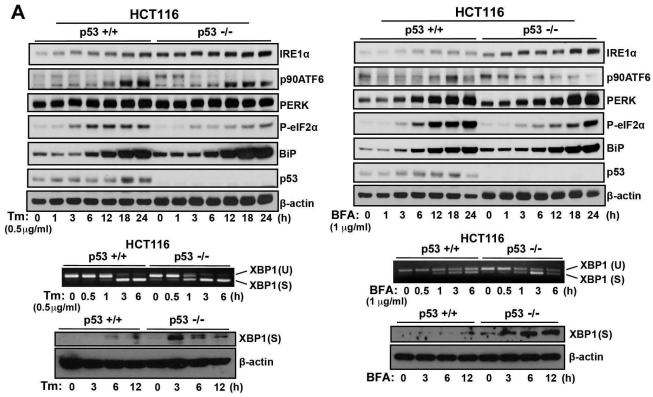

Western Blot

ER stress response in p53-deficient or knockdown cells. A.) HCT116 p53+/+ or HCT116 p53−/− cells, B. MEF p53+/+ or MEF p53−/− cells, and C. U2OS shLuc or U2OS shp53 cells were incubated with Tm (0.5 μg/mL) or BFA (1 μg/mL) for the times indicated. Cell lysates were analyzed using western blotting with the indicated antibodies. The blot was cut based on the size of proteins or stripped. Total RNAs were extracted and subjected to RT-PCR analysis using specific primer sets for XBP1(U) and XBP1(S). Cell lysates were analyzed using western blotting with indicated antibodies. Figure provided by CiteAb. Source: Oncotarget, PMID: 26254280.

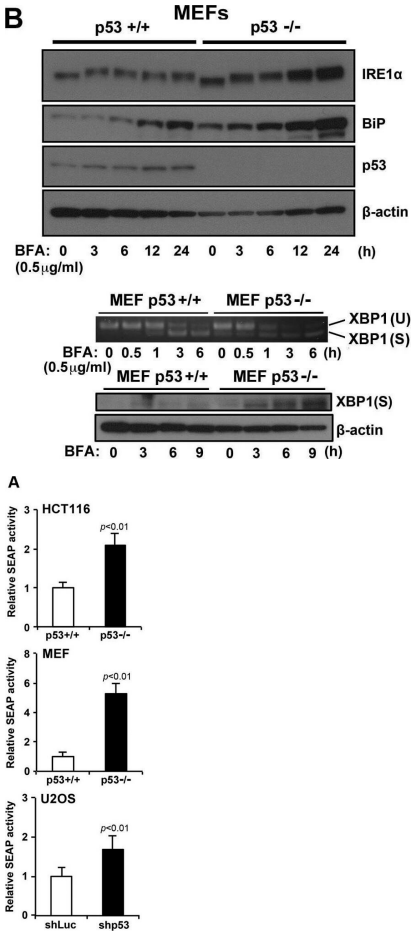

Western Blot

ER stress response in p53-deficient or knockdown cells. A.) HCT116 p53+/+ or HCT116 p53−/− cells, B.) MEF p53+/+ or MEF p53−/− cells, and C.) U2OS shLuc or U2OS shp53 cells were incubated with Tm (0.5 μg/mL) or BFA (1 μg/mL) for the times indicated. Cell lysates were analyzed using western blotting with the indicated antibodies. The blot was cut based on the size of proteins or stripped. Total RNAs were extracted and subjected to RT-PCR analysis using specific primer sets for XBP1(U) and XBP1(S). Cell lysates were analyzed using western blotting with indicated antibodies. Figure provided by CiteAb. Source: Oncotarget, PMID: 26254280.

Western Blot

p53 deficiency increases secretory the function of the ER through the IRE1α/XBP1 pathway. A.) HCT116 p53+/+ or HCT116 p53−/− cells, MEF p53+/+ or MEF p53−/− cells, and U2OS shLuc or U2OS shp53 cells expressing secreted embryonic alkaline phosphatase (SEAP) were transduced with a pSEAP2 control vector and washed 24 h after transduction. The medium was then changed, and the cells were cultured for another 6 h. Culture media were analyzed for SEAP activity, and luminescence was normalized to cell number. The transfection efficiencies of HCT116 p53+/+ and HCT116 p53−/− cells were approximately 80% each (data not shown). B.) Overexpression of wild-type p53 inhibited SEAP activity. SEAP activities of cells that constitutively expressed the indicated p53 molecules were analyzed using the same procedure described in (A). C.) HCT116 p53−/− cells that expressed SEAP were transfected with siControl, siATF6, siPERK, or siIRE1α, cultured for 24 h, and following a change of medium, the cells were cultured for another 6 h. Whole cell lysates were analyzed using western blotting with the indicated antibodies, and culture supernatants were analyzed for SEAP activity. Values shown are the mean ± s.d. of three different experiments simultaneously measured. The P value was calculated using two-way ANOVA. Figure provided by CiteAb. Source: Oncotarget, PMID: 26254280.

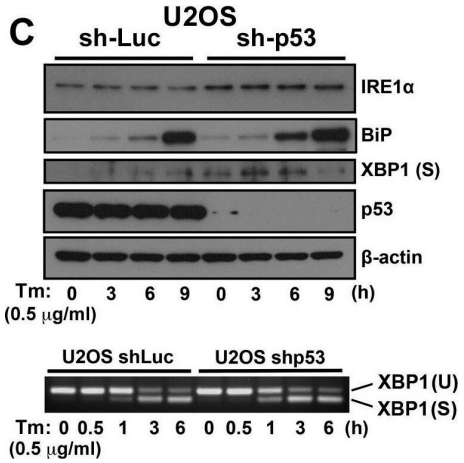

Western Blot

ER stress response in p53-deficient or knockdown cells. A.) HCT116 p53+/+ or HCT116 p53−/− cells, B. MEF p53+/+ or MEF p53−/− cells, and C. U2OS shLuc or U2OS shp53 cells were incubated with Tm (0.5 μg/mL) or BFA (1 μg/mL) for the times indicated. Cell lysates were analyzed using western blotting with the indicated antibodies. The blot was cut based on the size of proteins or stripped. Total RNAs were extracted and subjected to RT-PCR analysis using specific primer sets for XBP1(U) and XBP1(S). Cell lysates were analyzed using western blotting with indicated antibodies. Figure provided by CiteAb. Source: Oncotarget, PMID: 26254280.

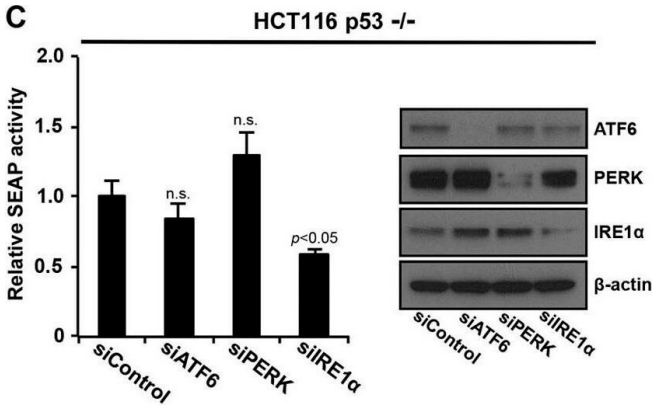

Western Blot

p53 deficiency increases secretory the function of the ER through the IRE1α/XBP1 pathway. A.) HCT116 p53+/+ or HCT116 p53−/− cells, MEF p53+/+ or MEF p53−/− cells, and U2OS shLuc or U2OS shp53 cells expressing secreted embryonic alkaline phosphatase (SEAP) were transduced with a pSEAP2 control vector and washed 24 h after transduction. The medium was then changed, and the cells were cultured for another 6 h. Culture media were analyzed for SEAP activity, and luminescence was normalized to cell number. The transfection efficiencies of HCT116 p53+/+ and HCT116 p53−/− cells were approximately 80% each (data not shown). B.) Overexpression of wild-type p53 inhibited SEAP activity. SEAP activities of cells that constitutively expressed the indicated p53 molecules were analyzed using the same procedure described in (A). C.) HCT116 p53−/− cells that expressed SEAP were transfected with siControl, siATF6, siPERK, or siIRE1α, cultured for 24 h, and following a change of medium, the cells were cultured for another 6 h. Whole cell lysates were analyzed using western blotting with the indicated antibodies, and culture supernatants were analyzed for SEAP activity. Values shown are the mean ± s.d. of three different experiments simultaneously measured. The P value was calculated using two-way ANOVA. Figure provided by CiteAb. Source: Oncotarget, PMID: 26254280.

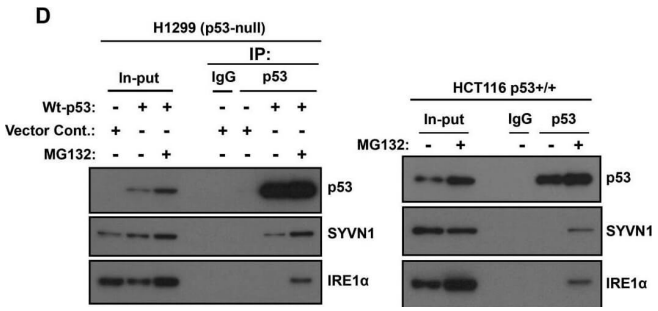

Western Blot

Synoviolin promotes IRE1α degradation in a wild-type p53-dependent manner. A.) SYVN1 suppresses IRE1α protein expression in wild-type p53 cells. HCT116 p53+/+ or HCT116 p53−/− cells were transfected with siControl (−) or siSYVN1 (+) and cultured for 24 h. Cell lysates were analyzed using western blotting with indicated the antibodies (left panel). The intensities of the SYVN1 bands were quantified. The levels of SYVN1 are reported relative to those of β-actin (right panel). The blot was cut based on the size of proteins or stripped and reprobed. B.) IRE1α and SYVN1 interaction is suppressed in p53-deficient cells. Proteins were cross-linked with DSP before protein extraction. Coimmunoprecipitation was performed with cell lysate using an IRE1α or an SYVN1 antibody. C.) SYVN1 interacts with wild-type p53. H1299 cells transiently expressed wild-type p53, p53-R248S, or p53-R273H. Coimmunoprecipitation experiments were performed using the anti-p53 antibody. D.) p53-SYVN1-IRE1α complex is observed by treatment with proteasome inhibitor. H1299 cells transiently expressing wild-type p53 (left panel) or HCT116 p53+/+ (right panel) cells were treated with 50 μM MG132 for 3 h. Coimmunoprecipitation experiments were performed using the anti-p53 antibody. Figure provided by CiteAb. Source: Oncotarget, PMID: 26254280.

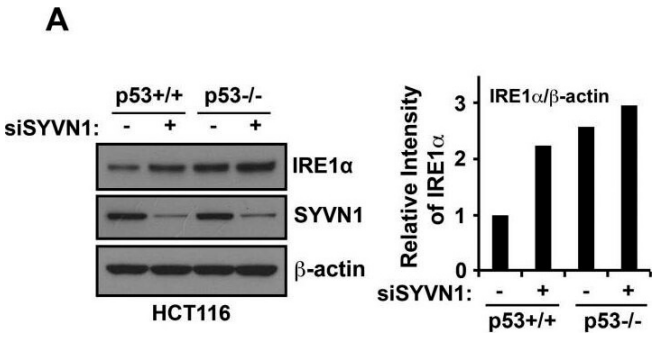

Western Blot

Synoviolin promotes IRE1α degradation in a wild-type p53-dependent manner. A.) SYVN1 suppresses IRE1α protein expression in wild-type p53 cells. HCT116 p53+/+ or HCT116 p53−/− cells were transfected with siControl (−) or siSYVN1 (+) and cultured for 24 h. Cell lysates were analyzed using western blotting with indicated the antibodies (left panel). The intensities of the SYVN1 bands were quantified. The levels of SYVN1 are reported relative to those of β-actin (right panel). The blot was cut based on the size of proteins or stripped and reprobed. B.) IRE1α and SYVN1 interaction is suppressed in p53-deficient cells. Proteins were cross-linked with DSP before protein extraction. Coimmunoprecipitation was performed with cell lysate using an IRE1α or an SYVN1 antibody. C.) SYVN1 interacts with wild-type p53. H1299 cells transiently expressed wild-type p53, p53-R248S, or p53-R273H. Coimmunoprecipitation experiments were performed using the anti-p53 antibody. D.) p53-SYVN1-IRE1α complex is observed by treatment with proteasome inhibitor. H1299 cells transiently expressing wild-type p53 (left panel) or HCT116 p53+/+ (right panel) cells were treated with 50 μM MG132 for 3 h. Coimmunoprecipitation experiments were performed using the anti-p53 antibody. Figure provided by CiteAb. Source: Oncotarget, PMID: 26254280.

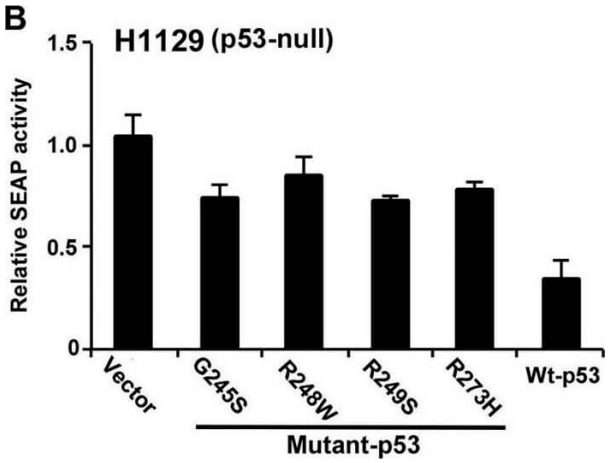

Western Blot

p53 deficiency increases secretory the function of the ER through the IRE1α/XBP1 pathway. A.) HCT116 p53+/+ or HCT116 p53−/− cells, MEF p53+/+ or MEF p53−/− cells, and U2OS shLuc or U2OS shp53 cells expressing secreted embryonic alkaline phosphatase (SEAP) were transduced with a pSEAP2 control vector and washed 24 h after transduction. The medium was then changed, and the cells were cultured for another 6 h. Culture media were analyzed for SEAP activity, and luminescence was normalized to cell number. The transfection efficiencies of HCT116 p53+/+ and HCT116 p53−/− cells were approximately 80% each (data not shown). B.) Overexpression of wild-type p53 inhibited SEAP activity. SEAP activities of cells that constitutively expressed the indicated p53 molecules were analyzed using the same procedure described in (A). C.) HCT116 p53−/− cells that expressed SEAP were transfected with siControl, siATF6, siPERK, or siIRE1α, cultured for 24 h, and following a change of medium, the cells were cultured for another 6 h. Whole cell lysates were analyzed using western blotting with the indicated antibodies, and culture supernatants were analyzed for SEAP activity. Values shown are the mean ± s.d. of three different experiments simultaneously measured. The P value was calculated using two-way ANOVA. Figure provided by CiteAb. Source: Oncotarget, PMID: 26254280.

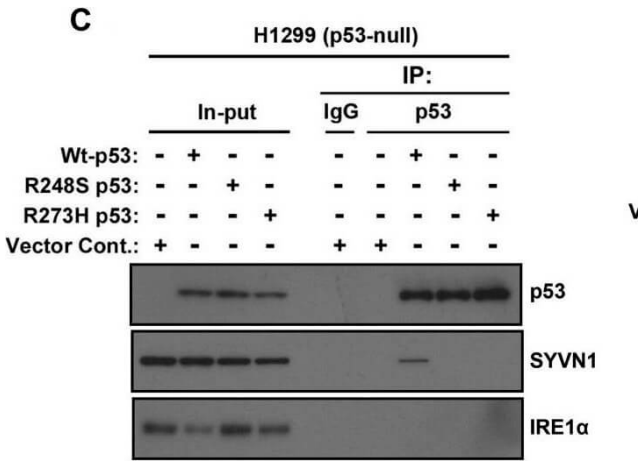

Western Blot

Synoviolin promotes IRE1α degradation in a wild-type p53-dependent manner. A.) SYVN1 suppresses IRE1α protein expression in wild-type p53 cells. HCT116 p53+/+ or HCT116 p53−/− cells were transfected with siControl (−) or siSYVN1 (+) and cultured for 24 h. Cell lysates were analyzed using western blotting with indicated the antibodies (left panel). The intensities of the SYVN1 bands were quantified. The levels of SYVN1 are reported relative to those of β-actin (right panel). The blot was cut based on the size of proteins or stripped and reprobed. B.) IRE1α and SYVN1 interaction is suppressed in p53-deficient cells. Proteins were cross-linked with DSP before protein extraction. Coimmunoprecipitation was performed with cell lysate using an IRE1α or an SYVN1 antibody. C.) SYVN1 interacts with wild-type p53. H1299 cells transiently expressed wild-type p53, p53-R248S, or p53-R273H. Coimmunoprecipitation experiments were performed using the anti-p53 antibody. D.) p53-SYVN1-IRE1α complex is observed by treatment with proteasome inhibitor. H1299 cells transiently expressing wild-type p53 (left panel) or HCT116 p53+/+ (right panel) cells were treated with 50 μM MG132 for 3 h. Coimmunoprecipitation experiments were performed using the anti-p53 antibody. Figure provided by CiteAb. Source: Oncotarget, PMID: 26254280.

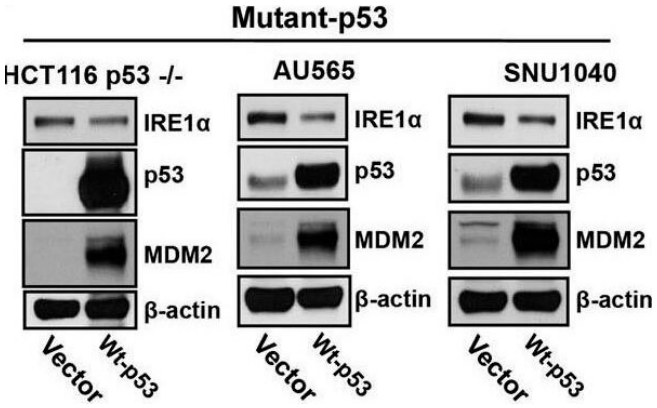

Western Blot

IRE1α expression is regulated by p53. A.) Western blot analysis of the expression of endogenous IRE1α in 23 human cancer cell lines. Cell lines were grouped according to expression of wild-type or mutant p53 as indicated. (A well between wt-p53 and mutant-p53 cell lines was cut, from the gel as indicated by a black line, due to the controversial p53 status of the cell line). Right panel: The intensities of the IRE1α bands (left panel) are expressed relative to those of β-actin. Values shown are the mean ± standard deviation (s.d.). The P value was calculated using two-way ANOVA. B.) Downregulation of p53 expression induces increased expression of IRE1α. HCT116 p53+/+ and U2OS cells were transfected with shLuc, shp53 (753), or shp53 (814), and selected using puromycin. Whole cell lysates of a pool of transfectants were analyzed using western blotting with the indicated antibodies. C.) Overexpression of wild-type p53 inhibits IRE1α expression in mutant-p53 cell lines. Cell lysates, prepared 48 h after transfection with wild-type p53, were analyzed for the expression of indicated proteins. D.) Mutant p53 proteins do not inhibit IRE1α expression. Cell lysates were prepared from cells transfected with p53-G245S, p53-R248W, p53-249S, and p53-R273H expression vectors or from cells that constitutively expressed wild-type p53 and were analyzed for the expression of the indicated proteins. Figure provided by CiteAb. Source: Oncotarget, PMID: 26254280.

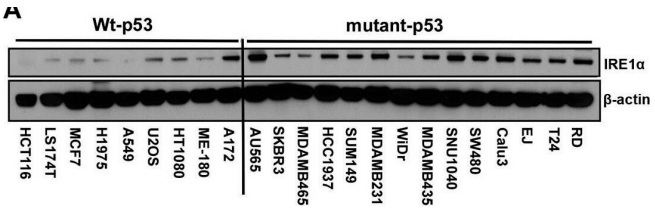

Western Blot

IRE1α expression is regulated by p53. A.) Western blot analysis of the expression of endogenous IRE1α in 23 human cancer cell lines. Cell lines were grouped according to expression of wild-type or mutant p53 as indicated. (A well between wt-p53 and mutant-p53 cell lines was cut, from the gel as indicated by a black line, due to the controversial p53 status of the cell line). Right panel: The intensities of the IRE1α bands (left panel) are expressed relative to those of β-actin. Values shown are the mean ± standard deviation (s.d.). The P value was calculated using two-way ANOVA. B.) Downregulation of p53 expression induces increased expression of IRE1α. HCT116 p53+/+ and U2OS cells were transfected with shLuc, shp53 (753), or shp53 (814), and selected using puromycin. Whole cell lysates of a pool of transfectants were analyzed using western blotting with the indicated antibodies. C.) Overexpression of wild-type p53 inhibits IRE1α expression in mutant-p53 cell lines. Cell lysates, prepared 48 h after transfection with wild-type p53, were analyzed for the expression of indicated proteins. D.) Mutant p53 proteins do not inhibit IRE1α expression. Cell lysates were prepared from cells transfected with p53-G245S, p53-R248W, p53-249S, and p53-R273H expression vectors or from cells that constitutively expressed wild-type p53 and were analyzed for the expression of the indicated proteins. Figure provided by CiteAb. Source: Oncotarget, PMID: 26254280.

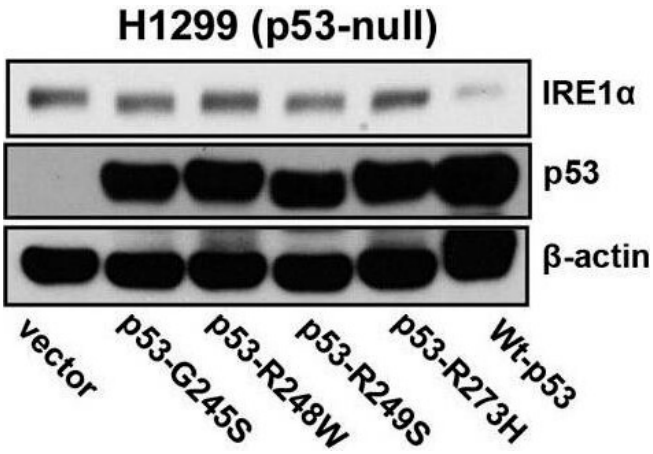

Western Blot

IRE1α expression is regulated by p53. A.) Western blot analysis of the expression of endogenous IRE1α in 23 human cancer cell lines. Cell lines were grouped according to expression of wild-type or mutant p53 as indicated. (A well between wt-p53 and mutant-p53 cell lines was cut, from the gel as indicated by a black line, due to the controversial p53 status of the cell line). Right panel: The intensities of the IRE1α bands (left panel) are expressed relative to those of β-actin. Values shown are the mean ± standard deviation (s.d.). The P value was calculated using two-way ANOVA. B.) Downregulation of p53 expression induces increased expression of IRE1α. HCT116 p53+/+ and U2OS cells were transfected with shLuc, shp53 (753), or shp53 (814), and selected using puromycin. Whole cell lysates of a pool of transfectants were analyzed using western blotting with the indicated antibodies. C.) Overexpression of wild-type p53 inhibits IRE1α expression in mutant-p53 cell lines. Cell lysates, prepared 48 h after transfection with wild-type p53, were analyzed for the expression of indicated proteins. D.) Mutant p53 proteins do not inhibit IRE1α expression. Cell lysates were prepared from cells transfected with p53-G245S, p53-R248W, p53-249S, and p53-R273H expression vectors or from cells that constitutively expressed wild-type p53 and were analyzed for the expression of the indicated proteins. Figure provided by CiteAb. Source: Oncotarget, PMID: 26254280.

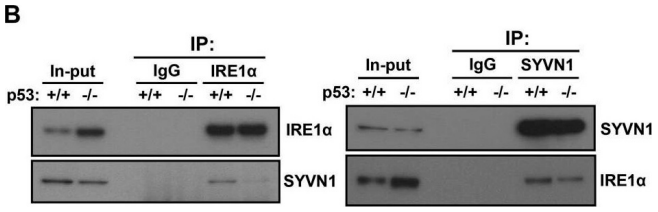

Western Blot

Synoviolin promotes IRE1α degradation in a wild-type p53-dependent manner. A.) SYVN1 suppresses IRE1α protein expression in wild-type p53 cells. HCT116 p53+/+ or HCT116 p53−/− cells were transfected with siControl (−) or siSYVN1 (+) and cultured for 24 h. Cell lysates were analyzed using western blotting with indicated the antibodies (left panel). The intensities of the SYVN1 bands were quantified. The levels of SYVN1 are reported relative to those of β-actin (right panel). The blot was cut based on the size of proteins or stripped and reprobed. B.) IRE1α and SYVN1 interaction is suppressed in p53-deficient cells. Proteins were cross-linked with DSP before protein extraction. Coimmunoprecipitation was performed with cell lysate using an IRE1α or an SYVN1 antibody. C.) SYVN1 interacts with wild-type p53. H1299 cells transiently expressed wild-type p53, p53-R248S, or p53-R273H. Coimmunoprecipitation experiments were performed using the anti-p53 antibody. D.) p53-SYVN1-IRE1α complex is observed by treatment with proteasome inhibitor. H1299 cells transiently expressing wild-type p53 (left panel) or HCT116 p53+/+ (right panel) cells were treated with 50 μM MG132 for 3 h. Coimmunoprecipitation experiments were performed using the anti-p53 antibody. Figure provided by CiteAb. Source: Oncotarget, PMID: 26254280.

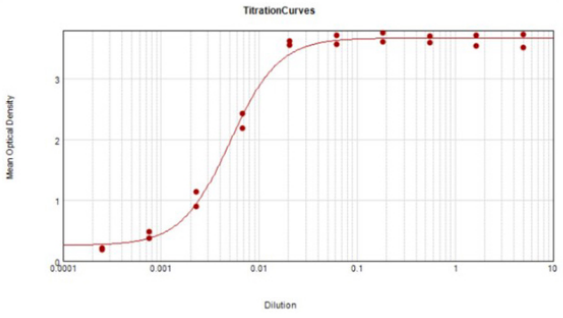

ELISA

ELISA Results of Mouse TrueBlot® ULTRA: Anti-Mouse Ig HRP. Each well was coated in duplicate with 1.0 μg of Mouse TrueBlot® ULTRA: Anti-Mouse Ig HRP (red line). The starting dilution of antibody was 5μg/ml and the X-axis represents the Log10 of a 3-fold dilution. The titer is 199,000. This titration is a 4-parameter curve fit where the IC50 is defined as the titer of the antibody. Assay performed using TMB-1000 substrate.

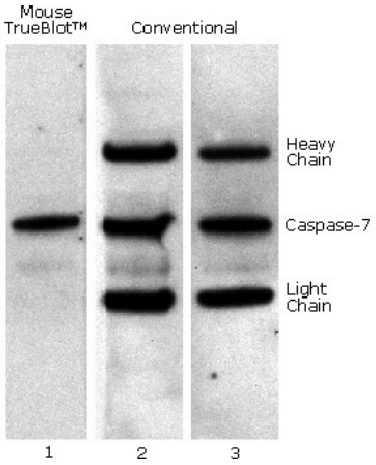

Western Blot
Mouse TrueBlot® IP / Western Blot: Caspase 7 was immunoprecipitated from 0.5 ml of 1x10e7 Jurkat cells/ml with 5 ug mouse anti-human Caspase 7. Precipitate from 1x10e6 cells was subjected to electrophoresis, transferred to an PVDF membrane, and Western blotted with anti-Caspase 7 using Mouse TrueBlot® ULTRA: Anti-Mouse Ig HRP (Lane 1) or conventional HRP-conjugated anti-mouse antibody (Lane 2) - note the detection of the heavy and light chains of the immunoprecipitating antibody in Lane 2 but not in Lane 1. When Lane 1 is re-immunoblotted using conventional HRP-conjugated anti-mouse polyclonal antibody (Lane 3), the heavy and light chains are now detected, confirming that although the immunoprecipitating heavy and light chains are present, Mouse TrueBlot® ULTRA: Anti-Mouse Ig HRP detects only native antibody and not denatured heavy and light chains.

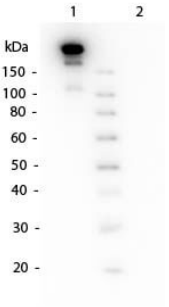

Western Blot
Western Blot of Mouse TrueBlot® ULTRA: Anti-Mouse Ig HRP. Lane 1: Mouse IgG, non-denatured. Center Lane: 5 µL Opal Pre-stained Ladder (p/n MB210-0500). Lane 2: Mouse IgG, denatured. Load: 50 ng. Primary antibody: none. Secondary antibody: Mouse TrueBlot® ULTRA: Anti-Mouse Ig HRP at 1:1,000 for 60 min at RT. Block: MB-070 for 30 min at RT. Predicted/Observed size: >160 kDa non-denatured for Mouse IgG.

References

- Lin LL et al. SEL1L-HRD1 interaction is required to form a functional HRD1 ERAD complex. *Nat Commun.* (2024)
- Wang HH et al. Hypomorphic variants of SEL1L-HRD1 ER-associated degradation are associated with neurodevelopmental disorders. *J Clin Invest.* (2024)
- Atarashi N et al. Activation of innate immune receptor TLR9 by mitochondrial DNA plays essential roles in the chemical long-term depression of hippocampal neurons. *J Biol Chem.* (2024)
- Maroni G et al. Tumor Microenvironment Landscapes Supporting EGFR-mutant NSCLC Are Modulated at the Single-cell Interaction Level by Unesbulin Treatment. *Cancer Res Commun.* (2024)
- Kawahara K et al. Truncated GPNMB, a microglial transmembrane protein, serves as a scavenger receptor for oligomeric β-amyloid peptide1-42 in primary type 1 microglia. *J Neurochem.* (2024)

- Knowles S et al. Conditional Depletion of STN1 in Mouse Embryonic Fibroblasts. *Bio Protoc.* (2024)
- Jones VT et al. Inhibition of autocrine HGF maturation overcomes cetuximab resistance in colorectal cancer. *Cell Mol Life Sci.* (2024)
- Surana S et al. The tyrosine phosphatase LAR acts as a receptor of the nidogen-tetanus toxin complex. *bioRxiv Preprint* (2023)
- Jin D et al. α2δ-1 protein drives opioid-induced conditioned reward and synaptic NMDA receptor hyperactivity in the nucleus accumbens. *J Neurochem.* (2023)
- Pappas G et al. MDC1 maintains active elongation complexes of RNA polymerase II. *Cell Rep.* (2023)
- Gong L et al. AKT Phosphorylates FAM13A and Promotes Its Degradation via CUL4A/DDB1/DCAF1 E3 Complex. *Am J Repair Cell Mol Biol.* (2023)
- Boehm D et al. The lysine methyltransferase SMYD5 amplifies HIV-1 transcription and is post-transcriptionally upregulated by Tat and USP11. *Cell Rep.* (2023)
- Refaat AM et al. HNRNPU facilitates antibody class-switch recombination through C-NHEJ promotion and R-loop suppression. *Cell Rep.* (2023)
- Chauhan C et al. PRMT5-mediated regulatory arginine methylation of RIPK3. *Cell Death Discov.* (2023)
- Bronkhorst AW et al. An extended Tudor domain within Vreteno interconnects Gtsf1L and Ago3 for piRNA biogenesis in Bombyx mori. *EMBO J.* (2023)
- Nguyen DD et al. Deficiency in mammalian STN1 promotes colon cancer development via inhibiting DNA repair. *Sci Adv.* (2023)
- Dailey-Krempel B et al. A tug of war between DCC and ROBO1 signaling during commissural axon guidance. *Cell Rep.* (2023)
- Muñoz-Reyes D et al. The neuronal calcium sensor NCS-1 regulates the phosphorylation state and activity of the Gα chaperone and GEF Ric-8A. *Elife.* (2023)
- Fang Z et al. Aurora A polyubiquitinates the BRCA1-interacting protein OLA1 to promote centrosome maturation. *Cell Rep.* (2023)
- Cross T et al. RNA Profiles of Tear Fluid Extracellular Vesicles in Patients with Dry Eye-Related Symptoms. *Int J Mol Sci.* (2023)
- Watanabe S et al. Skeletal muscle releases extracellular vesicles with distinct protein and microRNA signatures that function in the muscle microenvironment. *PNAS Nexus.* (2022)
- Walker AK et al. Modification of the SUMO activating enzyme subunit SAE2 directs SUMO isoform bias required for mitotic fidelity. *bioRxiv Preprint* (2022)
- Zhang, Z et al. Structure of SARS-CoV-2 membrane protein essential for virus assembly. *Nature Communications* (2022)
- Gao, Y et al. Pyrroloquinoline quinone (PQQ) protects mitochondrial function of HEI-OC1 cells under premature senescence. *Npj Aging* (2022)
- Xiang, Q et al. STAT and Janus kinase targeting by human herpesvirus 8 interferon regulatory factor in the suppression of type-I interferon signaling. *PloS Pathogens* (2022)

- Lankford, C et al. Identification of HCN1 as a 14-3-3 client. *PloS One* (2022)
- Gayatri, MB et al. High glutamine suppresses osteogenesis through mTORC1-mediated inhibition of the mTORC2/AKT-473/RUNX2 axis. *Cell Death Discovery* (2022)
- Niewolik, D et al. Physical ARTEMIS:DNA-PKcs interaction is necessary for V(D)J recombination. *Nucleic Acids Research* (2022)
- Matsuda, Y et al. Phosphorylation of hTERT at threonine 249 is a novel tumor biomarker of aggressive cancer with poor prognosis in multiple organs. *The Journal of Pathology* (2022)
- Alerasool N et al. Identification and functional characterization of transcriptional activators in human cells. *Mol Cel.* (2022)
- Shen JZ et al. A FBXO7/EYA2-SCFFBXW7 axis promotes AXL-mediated maintenance of mesenchymal and immune evasion phenotypes of cancer cells. *Mol Cell.* (2022)
- Liang G et al. CTNNBL1 restricts HIV-1 replication by suppressing viral DNA integration into the cell genome. *Cell Rep.* (2022)
- Cha SJ et al. Therapeutic modulation of GSTO activity rescues FUS-associated neurotoxicity via deglutathionylation in ALS disease models. *Dev Cell.* (2022)
- Lahree A et al. Active APPL1 sequestration by Plasmodium favors liver-stage development. *Cell Rep.* (2022)
- Huang X et al. A TET1-PSPC1-Neat1 molecular axis modulates PRC2 functions in controlling stem cell bivalency. *Cell Rep.* (2022)
- Zeng LW et al. The membrane-associated ubiquitin ligases MARCH2 and MARCH3 target IL-5 receptor alpha to negatively regulate eosinophilic airway inflammation. *Cell Mol Immunol.* (2022)
- Volkmar N et al. Regulation of membrane fluidity by RNF145-triggered degradation of the lipid hydrolase ADIPOR2. *EMBO J.* (2022)
- Desjardins P et al. The WNK1 kinase regulates the stability of transcription factors during wound healing of human corneal epithelial cells. *J Cell Physiol.* (2022)
- Namba Y et al. Maelstrom functions in the production of Siwi-piRISC capable of regulating transposons in Bombyx germ cells. *iScience.* (2022)
- Sarodaya N et al. Deubiquitinase USP19 enhances phenylalanine hydroxylase protein stability and its enzymatic activity. *Cell Biol Toxicol.* (2022)
- Saha B et al. Interactomic analysis reveals a homeostatic role for the HIV restriction factor TRIM5α in mitophagy. *Cell Rep.* (2022)
- Banerjee Sle et al. EPH receptor tyrosine kinases phosphorylate the PAR-3 scaffold protein to modulate downstream signaling networks. *Cell Rep.* (2022)
- Kucharski TJ et al. Small changes in phospho-occupancy at the kinetochore-microtubule interface drive mitotic fidelity. *J Cell Biol.* (2022)
- Sarodaya N et al. Deubiquitinase USP19 extends the residual enzymatic activity of phenylalanine hydroxylase variants. *Sci Rep.* (2022)

- Al-Habsi M et al. Spermidine activates mitochondrial trifunctional protein and improves antitumor immunity in mice. *Science.* (2022)
- McCool MA et al. Human pre-60S assembly factors link rRNA transcription to pre-rRNA processing. *RNA.* (2022)
- Malgorzata Bodaszewska-Lubas et al. Dominant-Negative Form of SIGIRR: SIGIRRΔE8 Promotes Tumor Growth Through Regulation of Metabolic Pathways. *J Interferon Cytokine Res.* (2022)
- Aso M et al. First-in-human autologous implantation of genetically modified adipocytes expressing LCAT for the treatment of familial LCAT deficiency. *Heliyon.* (2022)
- Blue SM et al. Transcriptome-wide identification of RNA-binding protein binding sites using seCLIP-seq. *Nat Protoc.* (2022)
- View More ...

Disclaimer